

Printing Ultrathin Graphene Oxide Nanofiltration Membranes for Water Purification

Mahdi Fathizadeh,^a Huynh Ngoc Tien,^a Konstantin Khivantse,^a Jung-Tsai Chen^a and Miao

Yu^{b}*

^aDepartment of Chemical Engineering and Catalysis for Renewable Fuels Center, University of South Carolina, Columbia, SC 29208, USA

^bDepartment of Chemical and Biological Engineering, Rensselaer Polytechnic Institute, Troy, NY 12180, USC

*Corresponding author: yum5@rpi.edu

1. Large graphene oxide (GO) flake preparation and characterization

Large, single-layered GO flakes were synthesized following previous studies and characterized thoroughly by FT-IR and XPS for surface functional groups and elemental compositions thickness and AFM for the size and thickness of GO sheets.^{1,2} Note the 2nd author (Huynh Ngoc Tien) of this study, who prepared large GO flakes, is the 1st author of references [1] and [2]. The experimental procedure was described briefly as follows. Expandable graphite was firstly heated for 30 s in a microwave oven to obtain expanded graphite. Graphene oxide was synthesized from the expanded graphite using modified Hummers method. 500 mL of concentrated H₂SO₄ was charged into 3-L flask equipped by mechanical stirrer. The ice bath was used to decrease flask temperature to around 0 °C. Five grams of expanded graphite were slowly added into flask under stirring. Then, 30 g of KMnO₄ was gradually added to expanded graphite suspension and mixed for 2 h at 35 °C. The flask was then chilled again in the ice bath, and 1 L of deionized water was slowly added to maintain a temperature below 70 °C. Fifty ml of H₂O₂ (30 wt%) was added to

suspension, and the color of suspension changed from dark brown to yellow. The oxidized product was purified by rinsing with a 5% HCl solution and repeatedly washing with DI water.

2. Membrane thickness calculation

From HP printer Company website (<http://store.hp.com/us/en/pdp/hp-63-black-original-ink-cartridge>), the volume of each ink drop of cartridge 63 is around 22×10^{-12} L. Moreover, each drop covers an average surface area of $90 \times 1,000 \mu\text{m}^2$, as shown in Fig. S1. Therefore,

1- Liquid volume/Membrane surface = 22×10^{-12} (L drop⁻¹) / $[(90 \times 1000 \times 10^{-12}) (\text{m}^2 \text{ drop}^{-1})]$ = $0.000244 \text{ L m}^{-2} = 0.00244 (\text{cm}^3 \text{ cm}^{-2})$ or (ml cm^{-2})

2- For GO “ink” with concentration of 1 mg ml^{-1} , GO loading per area = $0.00244 (\text{ml cm}^{-2}) \times 1 (\text{mg ml}^{-1}) = 0.00244 (\text{mg cm}^{-1})$

3- Assuming GO density of $1.8 (\text{g cm}^{-3})$, GO coating thickness will be $0.00244 (\text{mg cm}^{-2}) / 1.8 (\text{g cm}^{-3}) = 1.36 \times 10^{-6} (\text{cm}^3 \text{ GO} / \text{cm}^2 \text{ membrane surface}) = 1.36 \times 10^{-6} \text{ cm}$

4- GO coating thickness after one-time printing using 1 mg ml^{-1} GO “ink” = $1.36 \times 10^{-6} \text{ cm} \times 10^7 \text{ nm cm}^{-1} = 13.6 \text{ nm}$.

5- GO coating thickness after one-time printing using GO “ink” at difference concentrations can be calculated following the above procedure.

2. Membrane permeation and rejection measurements

Lab-scale dead-end and cross-flow systems (Fig. S9) were used to measure the water flux through printed GO membranes. A stainless steel dead-end module (Sterlitech HP4750) with effective permeation area of 5.1 cm^2 was used for filtration test. As shown in Fig. S9, feed side can be pressurized by nitrogen cylinder from 68.9 to 689.5 kPa Pure water permeation experiment was

performed at room temperature and feed pressure of around 68.9 kPa for 1 h. Moreover, nanofiltration performance of printed GO membranes was tested using charged and uncharged dyes with different molecular diameters and neutral pharmaceutical components. The permeability of membrane for dye solution and pharmaceutical components was determined at feed pressure around 206.8 kPa for 2 h, and calculated by:

$$\text{Permeability} = \frac{V_p}{t.A.\Delta P}$$

where V_p , t , A , and ΔP are the permeate volume (L), time (h), membrane area (m^2), and pressure drop (bar). Rejection (R) was calculated by:

$$R (\%) = 1 - \frac{C_p}{C_f}$$

where C_p and C_f are the contaminant concentration in permeate and feed, respectively. Feed concentration of dye and pharmaceutical components were 0.02 mM and 10 ppm, respectively. Also, the concentration of dye and pharmaceutical components were measured by UV-vis spectroscopy (UV-2600 Shimadzu, Japan) and Total organic carbon (TOC) (Tekmar Phoenix 8000-Persulfate), respectively.

Salt rejection of fabricated GO membranes was evaluated using 2 g/l of monovalent and divalent salts, such as NaCl, MgCl₂, MgSO₄, and Na₂SO₄ at pressure 344.7 and 482.6 kPa. Concentration of salts in permeant side was measured by a conductivity meter (Pour Grainger International, Lake Forest, IL, USA).

For long time testing, a cross-flow system (Fig. S9), with membrane area around 20 cm², was used to evaluate the stability of printed GO membrane for rejection of dyes and pharmaceutical components for 1,500 min. The feed solution was circulated and pressurized with peristaltic pump

at room temperature with pressure drop around 206.8 kPa. The permeate side was equipped with a balance for recording the permeate weight.

UV-visible spectroscopy. UV-visible spectroscopy was used for measuring the concentration of dye solutions in the permeate and retentate.

3. Characterization

The fabricated GO membranes were characterized by Atomic Force Microscopy (AFM), Contact angle (CA), Field Emission Scanning Electron Microscope (FESEM), and Fourier transform infrared spectroscopy-Attenuated total reflection (FTIR-ATR).

Atomic Force Microscopy (AFM). AFM images were scanned by TT-AFM system purchased from AFM workshop under vibration mode with a spatial resolution of approximately 0.15 nm in Z direction, and analyzed by Gwyddion 2.41. AFM was used to measure the change of membranes surface roughness (RMS) before and after printing GO layer. The instrument was calibrated by standard samples. 5 μm \times 5 μm areas of three different location were fixed on holder with double-sided tape, were measured in the air and room temperature. The average roughness was reported

Contact angle. Contact angle and advancing contact angle of water and GO solution on surface of PAN and M-PAN were analyzed by Ramé-Hart contact angle goniometer (Succasunna, NJ). Water CA was measured at 25 °C with distilled water for several different spots of membrane surface, and the average values were reported as the CA of the prepared membranes.

Field Emission Scanning Electron Microscope (FESEM). FESEM images were taken using a Zeiss ultraplus thermal field emission scanning electron microscope and with gold coating. FESEM

analysis for investigating the morphology of the membrane surface and finding the thickness of GO layer. For cross section, the GO membranes were fractured by immersing them into liquid nitrogen. Then, double side copper tape was used to stick prepared samples on a conducting sample holder. The prepared samples were coated under vacuum with gold sputtering for 45 sec.

Fourier transform infrared spectroscopy-Attenuated total reflection (FTIR-ATR). FTIR-ATR experiments were performed on a Thermo Scientific, Waltham, MA, USA which coupled to a ZnSe ($n_1=2.43$) prism as an internal reflection element and was fixed at a 60° angle of incidence with 2 cm^{-1} resolution over a wave number range of $600\text{--}4000\text{ cm}^{-1}$. We did FTIR-ATR analysis on PAN and M-PAN membranes to study the difference of functional groups on surface of modified/unmodified PAN supports. To detect the difference between modified and unmodified membranes, the dry membranes without further treatment and the hydrolyzed membranes were cut into the size of $1\text{ cm}\times 1\text{ cm}$, and used for FTIR analysis. To minimize the error each sample was scanned 4 times and the average value was reported.

4. Viscosity measurement:

Viscosity of GO dispersion was measured at ambient temperature using a glass capillary viscometer (50 L199, Cannon Instrument Company). The glass capillary viscometers were filled with the GO dispersion by using suction to pull solution to the upper mark of calibrated volume inside of the viscometer. Flowing time of the liquid down to the lower calibrated mark of the glass viscometer was measured. The provided calibration constant by the manufacture was used to calculate the viscosity of GO “ink” solutions. The viscosity of GO “ink” solution as a function of GO concentration was shown in Fig. S2.

Table S1. MO rejection of commercial nanofiltration membranes.

Membrane	Type	MWCO (Daltons)	MO Rejection (%)
Microdyn Nadir	TS40	500	15.8
TriSep	NP030	200	37.7
Dow Filmtec	NF90	200-400	75.6

Table S2. Water flux and Sal/dye rejection of GO membranes

Deposition method	Thickness (nm)	Permeance ($L\ m^{-2}h^{-1}bar^{-1}$)	Rejection	Reference
Layer by layer	40-90	2-8	70-90% (dye) 20-85% (salts)	4
Vacuum filtration	1500	12-70	80->99% (dye)	5
Casting high concentration GO	150	71±5	>90% (dye)	6
Vacuum filtration of reduced GO	22-53	21.8	> 99% (dye) 20-60% (salts)	7
Vacuum filtration	4.7-100	0.1-20	10-65% (salts)	8
Printing	7.5-60	15-85	20-60% (salts) 85->99% (dye)	This work

Table S3. Rejection of 4 pharmaceutical components using printed GO membrane (30 nm and two-time printing).

Pharmaceutical component	Molecular weight (g/mol)	Rejection, %
Gemfibrozil	250.33	76.4
17 a-Ethynylestradiol	296.41	80.1
Diclofenac Sodium Salt	318.13	83.0
Iodixanol	1550	95.2

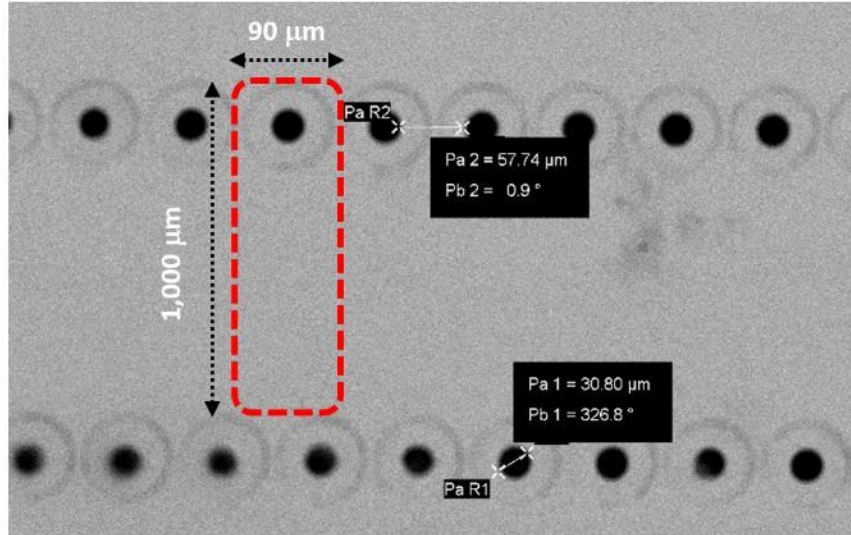


Figure S1. FESEM image of commercial HP ink cartridge nozzles. The black circles are the nozzle pores with diameter around 30 μm; distance between two holes in one row is about 90 μm; the distance between rows is about 100 μm. The average surface area for one drop is shown in the red dashed box.

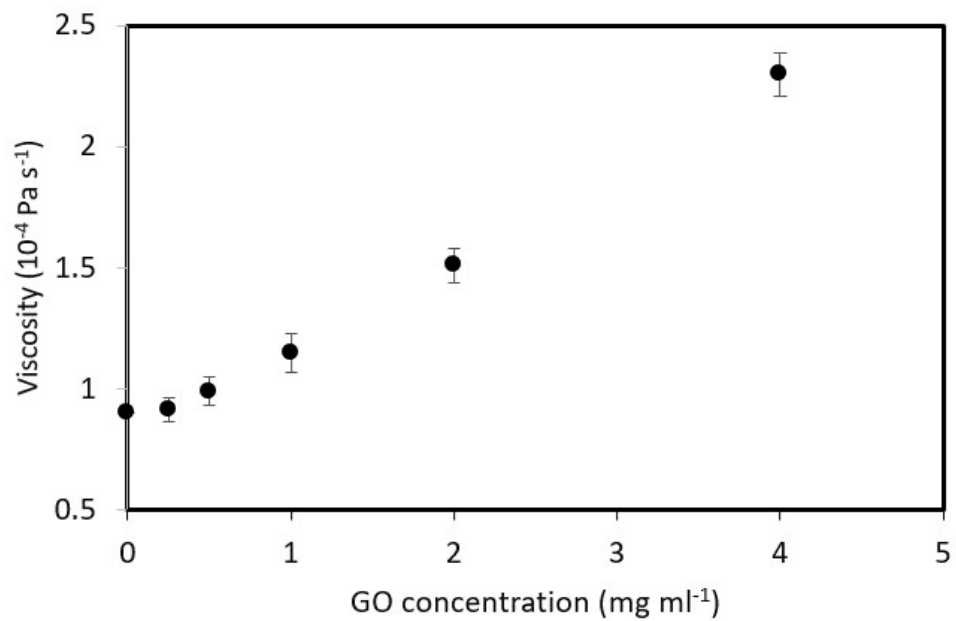


Figure S2. GO “ink” viscosity as a function of with GO concentration

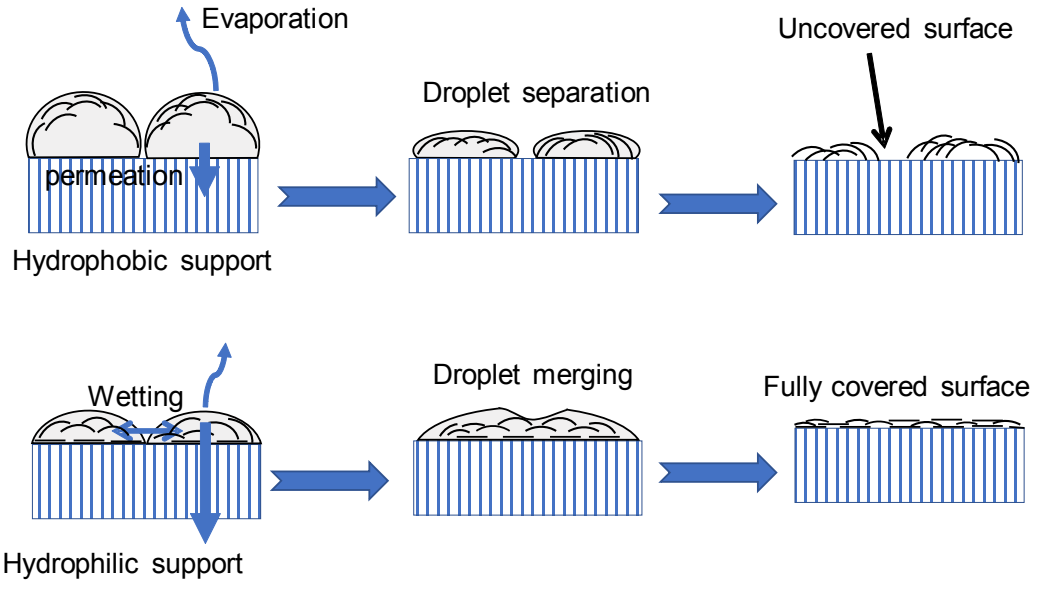


Figure S3: Proposed GO deposition mechanisms on hydrophobic and hydrophilic supports by printing method.

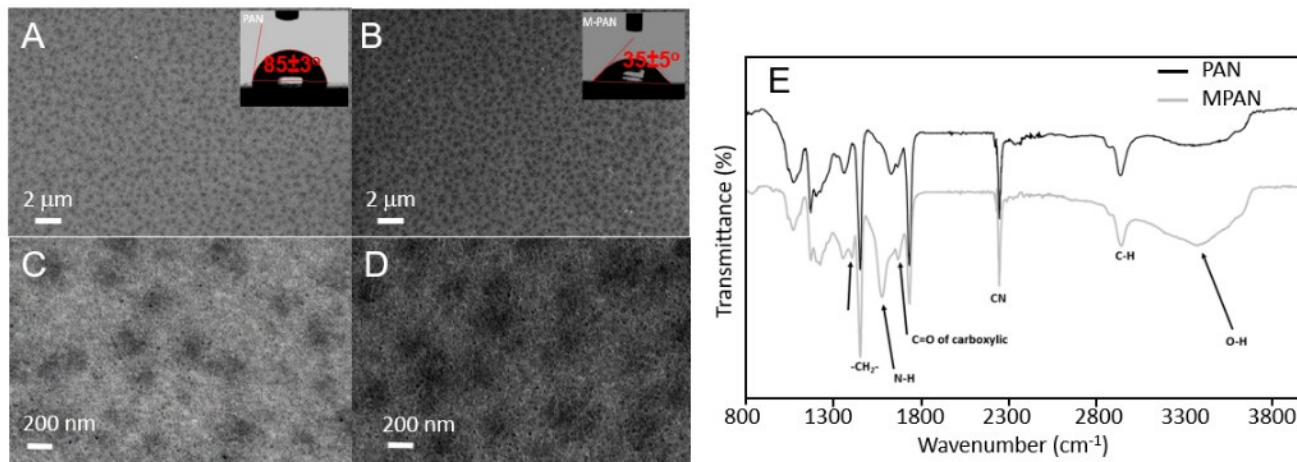


Figure S4: Characterization of PAN and M-PAN supports. FESEM images of PAN support at low (A) and high magnification (C); inset in (A) shows the water contact angle of PAN. FESEM images of M-PAN support at low (B) and high magnification (D); inset in (B) shows the water contact angle of M-PAN. FTIR-ATR spectra of PAN and M-PAN (E). The high magnification FESEM images of PAN and M-PAN show that the actual pore size of the top skin layer is around 20 to 50 nm; larger pores (~200 nm) below the top skin layer can also be seen due to the thin skin layer of PAN or M-PAN.

FTIR-ATR spectroscopy results clarify that the intensity of carboxylic group on M-PAN membrane increase with hydrolyzation reaction (Fig. S4). Comparing FTIR-ATR spectroscopy of PAN and M-PAN membranes shows that the intensity of -CN group peak at around 2243 cm^{-1} decreases after hydrolyzation, and creates new peaks at $3300\text{--}3400$, 1710 , and 1560 cm^{-1} correspond to -OH, and C=O of carboxylic, as well as -NH of amide II, respectively. FTIR-ATR result indicates clear evidence that the hydrolyzation reaction by sodium hydroxide solutions can produce carboxylic groups. This carboxylic acid group on M-PAN membrane surface and in side

of pores can absorb water from GO solution and increase the affinity of membrane surface with GO flakes.

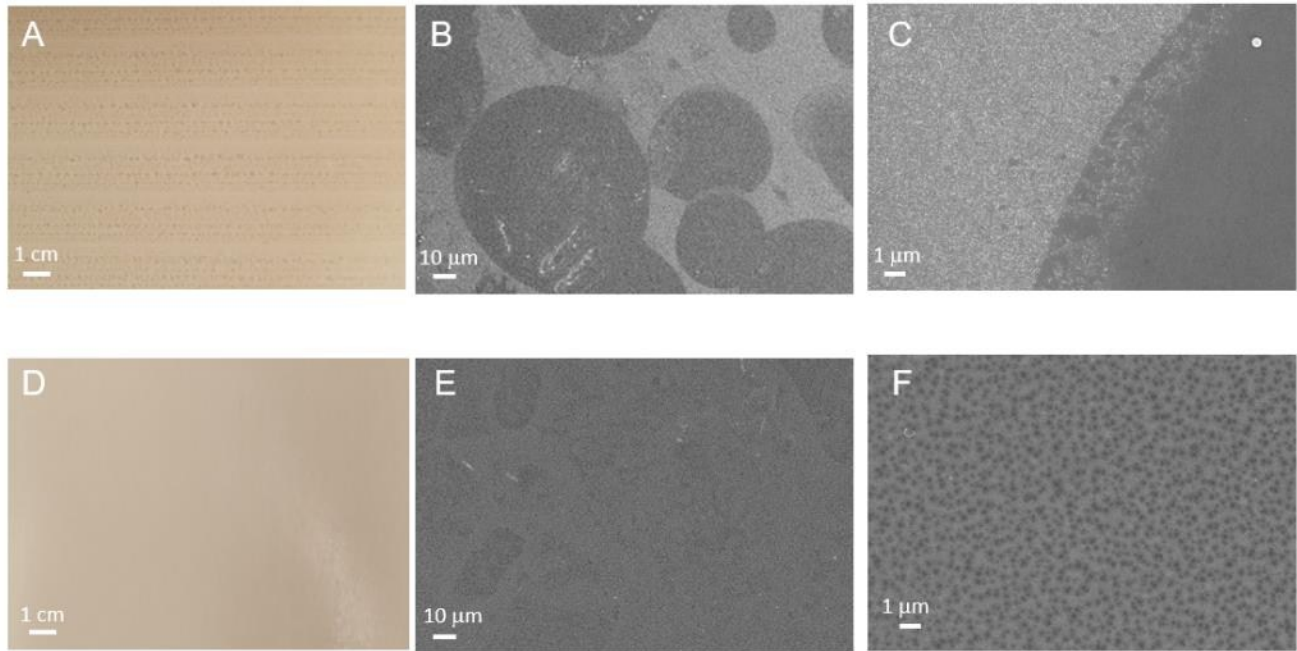


Figure S5: Characterization of the uniformity of printed GO coatings on PAN and modified-PAN (M-PAN) supports; digital picture (A) and FESEM images at lower (B) and higher (C) magnification of printed GO on PAN support; digital picture (D) and FESEM images at lower (E) and higher (F) magnification of printed GO on M-PAN support. Printing condition: GO concentration: 1 mg ml^{-1} ; one-time printing.

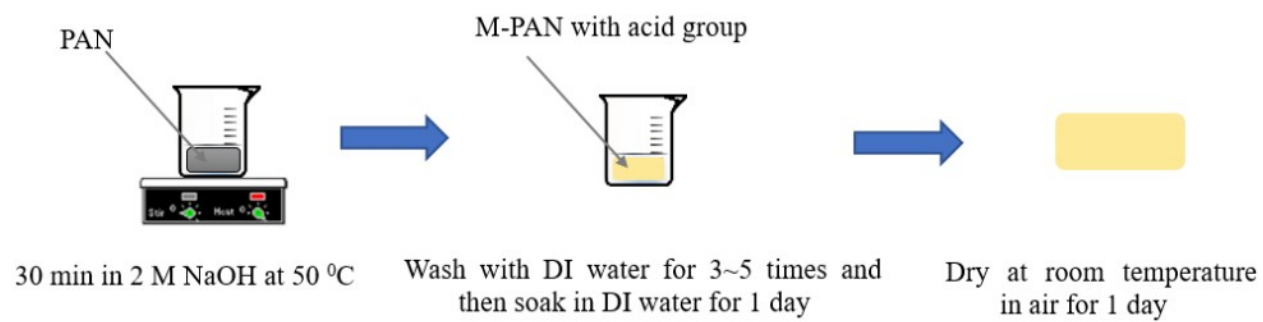


Figure S6: Modification Process for PAN support.

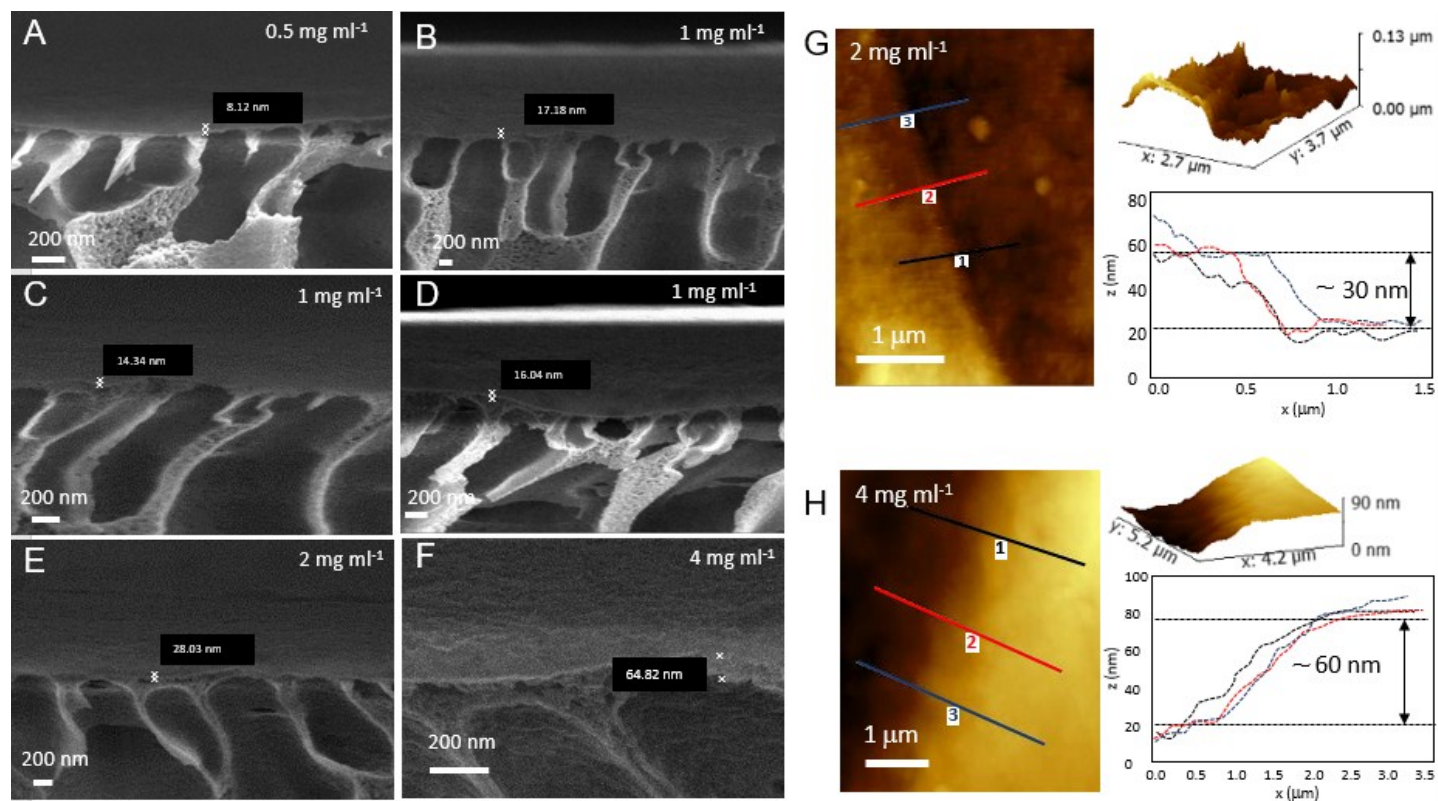


Figure S7: Characterization of thickness of printed GO coatings on M-PAN. Cross-sectional FESEM images of GO coatings on M-PAN printed using 0.5 (A), 1 (B, C, D), 2 (E) and 4 (F) mg ml⁻¹ GO “ink”; B, C and D are from three different printed membranes. AFM images of printed GO coatings using 2 (G) and 4 (H) mg ml⁻¹ GO “ink”; corresponding height profiles along three lines are also shown. Note: all these GO coatings are deposited by one-time printing.

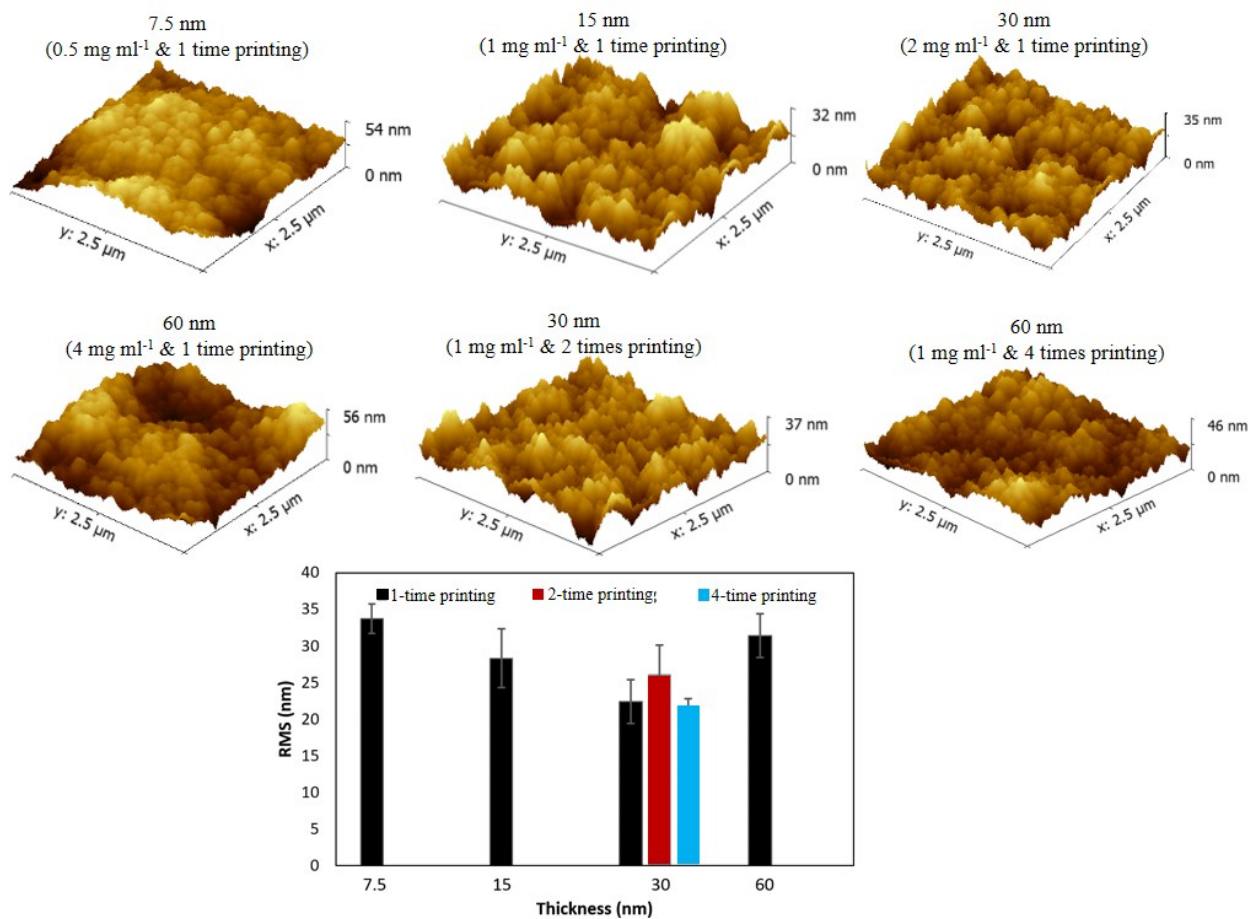


Figure S8: AFM images of GO coatings printed using different concentrations and different printing times, and surface roughness of printed GO coatings.

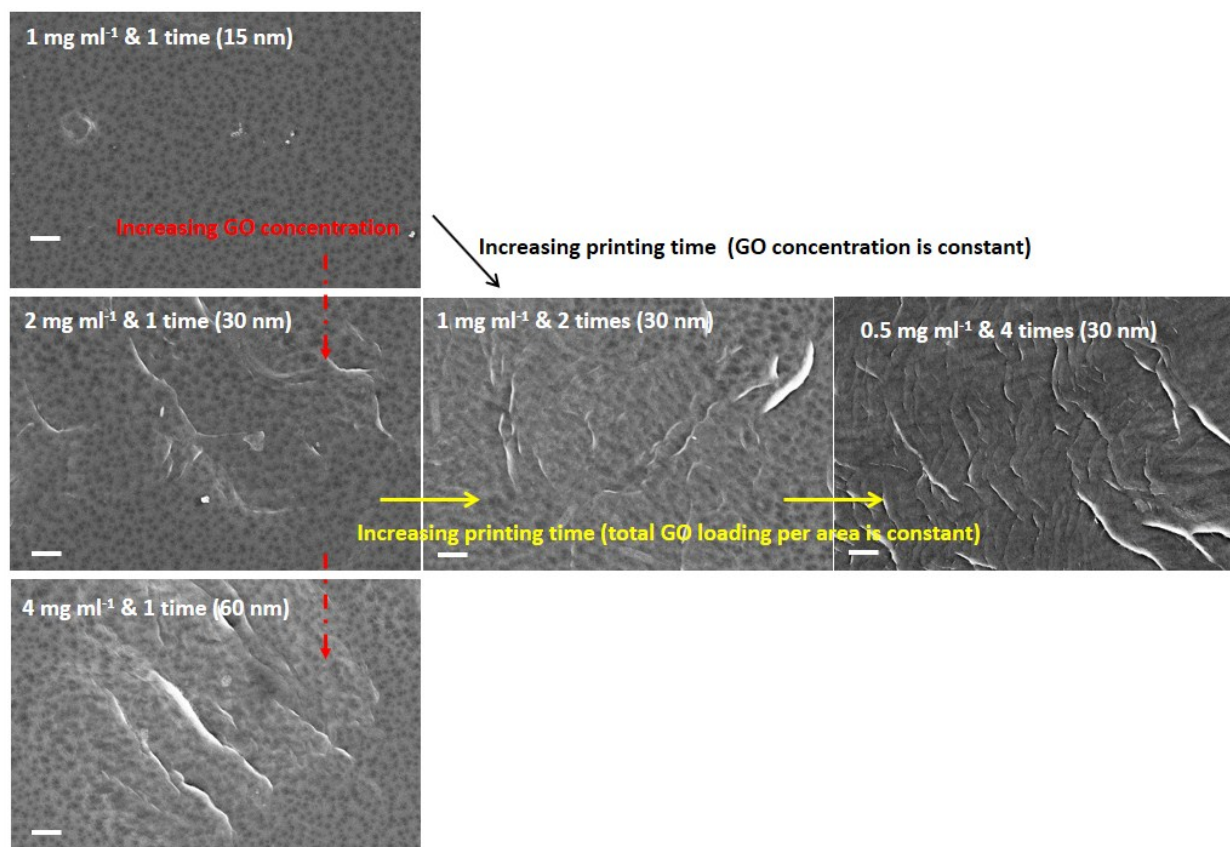
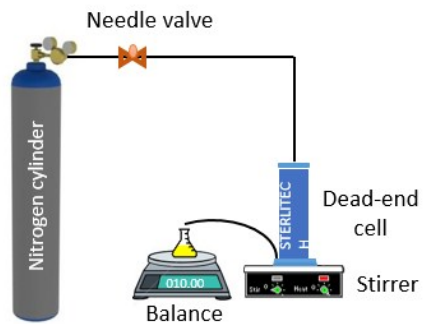


Figure S9: FESEM images of the surface of GO coatings printed using different GO concentrations and different printing times. Scale bar is 2 μm

Dead-end system



Cross-flow system

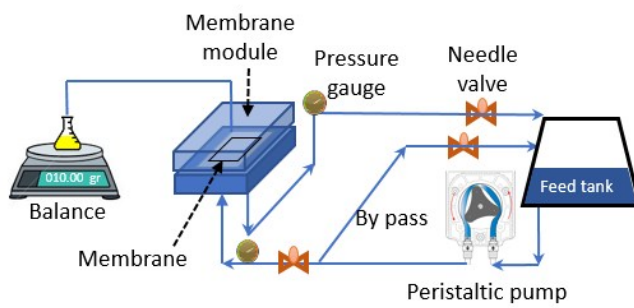


Figure S10: Experimental setup of water permeation and purification systems.

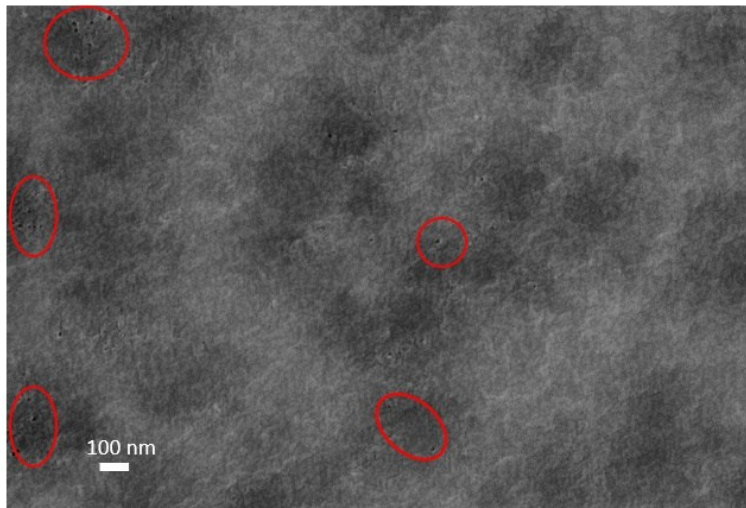


Figure S11: FESEM image of the surface of 7.5 nm GO coating. Red circles indicate exposed support pores.

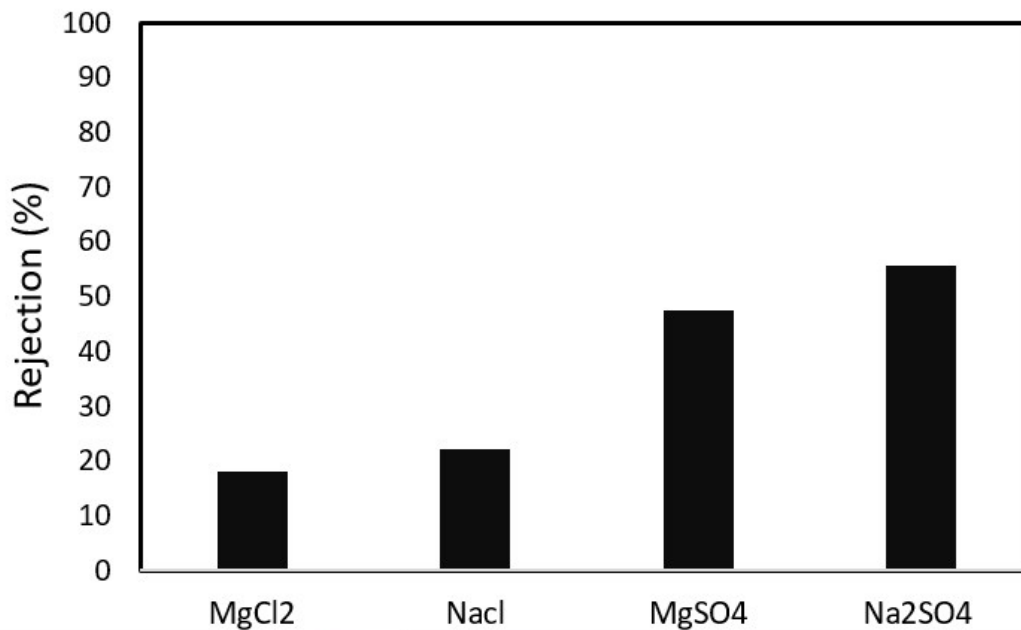


Figure S12: Salt rejection by 30 nm GO membrane by two-time printing. Feed applied pressure is 344.7 kPa.

Salt separation performance of the printed GO membranes was examined using 2 g/L salt solution of Na₂SO₄, MgSO₄, NaCl and MgCl. Note that PAN and M-PAN support have no rejection for both salts and MO. The fabricated GO membrane showed NaCl rejection between 9% to 28 % and 14% to 34 % at 344.7 and 482.6 kPa applied pressure, respectively. Previous studies showed that higher operating pressure can pack GO layer and improve salt rejection or dye rejection, which is in the good agreement with MD modeling studies. For mono and divalent salt rejection, fair rejection for Na₂SO₄ and MgSO₄, around 52% and 41%, was observed, while moderate rejection (22% and 18 %) of NaCl and MgCl was found for the printed GO membrane. The observed salt rejection can be ascribed to Donnan exclusion for negative charged GO membrane.

References

1. H. N. Tien, V. H. Luan, T. K. Lee, B. S. Kong, J. S. Chung, E. J. Kim and S. H. Hur, *Chem. Eng. J.*, 2012, **211**, 97-103.
2. H. N. Tien and S. H. Hur, *Phys Status Solidi-R*, 2012, **6**, 379-381.
3. D. A. Dikin, S. Stankovich, E. J. Zimney, R. D. Piner, G. H. B. Dommett, G. Evmenenko, S. T. Nguyen and R. S. Ruoff, *Nature*, 2007, **448**, 457-460.
4. Q. Nan, P. Li and B. Cao, *Appl Surf Sci*, 2016, **387**, 521-528.
5. H. B. Huang, Y. Y. Mao, Y. L. Ying, Y. Liu, L. W. Sun and X. S. Peng, *Chem Commun*, 2013, **49**, 5963-5965.
6. A. Akbari, P. Sheath, S. T. Martin, D. B. Shinde, M. Shaibani, P. C. Banerjee, R. Tkacz, D. Bhattacharyya and M. Majumder, *Nat Commun*, 2016, **7**.
7. Y. Han, Z. Xu and C. Gao, *Adv Funct Mater*, 2013, **23**, 3693-3700.
8. W. W. L. Xu, C. Fang, F. L. Zhou, Z. N. Song, Q. L. Liu, R. Qiao and M. Yu, *Nano Lett*, 2017, **17**, 2928-2933.